ARTICLES

Carbon Nanotube Bundles as Molecular Assemblies for the Detection of Polycyclic Aromatic Hydrocarbons: Surface-Enhanced Resonance Raman Spectroscopy and Theoretical Studies

P. Leyton,[†] J. S. Gómez-Jeria,[†] S. Sanchez-Cortes,*[,‡] C. Domingo,[‡] and M. Campos-Vallette[†]

Department of Chemistry, Faculty of Sciences, University of Chile, P. O. Box 635, Santiago, Chile, and Instituto de Estructura de la Materia, CSIC, Serrano, 121, 28006 Madrid, Spain

Received: November 4, 2005; In Final Form: February 16, 2006

In this work surface-enhanced resonance Raman spectroscopic experiments have demonstrated that metallic single-walled carbon nanotubes can be used as chemical assemblies between the pyrene analyte and the silver colloidal surface. Pyrene has been detected at concentrations lower than 10^{-9} M by use of the 514.5 nm excitation laser line. A charge transfer from the surface to the nanotube characterizes the nanotube−silver surface interaction. The pyrene−nanotube interaction occurs through a $\pi-\pi$ electronic stacking. Extended Hückel calculations based on a simplified molecular model for the analyte/nanotube/surface system support the experimental conclusions. The nanotube−pyrene distance is 3.4 Å, and the most probable orientation for pyrene is confirmed to be plane parallel to the nanotube surface. An energy transfer from the silver surface to the nanotube/analyte system is verified.

Introduction

Carbon nanotube (NT) composites represent a potentially significant advance in the field of preconcentration and analytical separations due to their high surface area and high thermal conductivity. These two characteristics suggest in particular that carbon nanotube composites could be used as preconcentrators to facilitate trace detection of contaminants. The high surface area of carbon nanotubes allows an effective miniaturization of the preconcentrators, while high thermal conductivity leads to their fast cycling. However, there is a lack of understanding of how the nanotube structure affects sorption properties, which is necessary for the design of an optimized preconcentrator.

In general, aromatic compounds such as anthracene, pyrene, and phthalocyanine derivatives interact with the graphitic walls of nanotubes.[1] Stacking of polycyclic aromatic hydrocarbons (PAHs) on nanotubes is a viable approach to functionalize carbon nanotubes through noncovalent bonding. This procedure has been employed to immobilize chemical and biochemical molecules on NTs.[2−4] On the other hand, the immobilization of PAHs on NTs is a process that can be applied in the design of sensitive and selective chemical sensors for these pollutants. Therefore, a full understanding of the interaction between NTs and PAHs is of interest under many points of view.

Since PAHs are dangerous contaminants and potentially carcinogenic,[5] it is important to detect them at very low concentrations. Surface-enhanced Raman scattering spectroscopy (SERS) is a useful and actual technique to identify small amounts of molecules adsorbed on metal surfaces. One of the most attractive characteristic of SERS, in analytical terms, is the possibility of reaching detection limits lower than 10^{-12} M, giving rise to single molecule detection spectroscopy. This technique also allows inferences about the orientation and molecular organization of analytes deposited onto a surface.

In previous works we have concluded that PAHs have no SERS spectra when directly deposited on metal surfaces.[6] However, the Raman enhancement of the PAHs pyrene and benzo[*c*]phenanthrene was obtained by using calixarenes as molecular assemblers (inclusion assemblers).[7] On the other hand, the SERS spectrum of nanotubes was reported by Corio et al.[8] by using different excitation laser lines and metal surfaces. From these studies it was evident that the Raman resonant effect of nanotubes can be applied to study their electronic characteristics.

Thus, one of the purposes of this work is to obtain insights about the physicochemical characteristics of the nanotube/PAH system. The other one is to detect PAHs at very low concentrations by using NT bundles as new molecular assemblies (contact assemblers) between the metallic surface and the analytes. Raman, Raman resonance spectroscopies, and surface-enhanced resonance Raman scattering (SERRS) techniques were used to achieve these objectives. We have chosen pyrene as a molecular model since it is well characterized and because of its simple structure. To complete the interpretation of the spectroscopic results, we performed extended Hückel calculations of some simple molecular models in which pyrene interacts with one and two (5,5) armchair single-walled metallic nanotubes, the whole deposited on a silver surface.

The understanding of the analyte/NT/surface interaction should be useful for establishing analytical applications of the whole system in the field of optical environmental sensors.

* To whom correspondence should be addressed. Phone: + 34 91 5 61 68 00. Fax: + 34 91 5 64 55 57. E-mail: imts158@iem.cfmac.csic.es.
[†] University of Chile.
[‡] Instituto de Estructura de la Materia.

10.1021/jp056379z CCC: $33.50
Published on Web 03/16/2006

Experimental Section

Pyrene (PYR) was purchased from Merck and used as received. Solutions of this compound in acetone (99%) were prepared to a final concentration of 10^{-2} M. The lowest concentrations (10^{-9} M) were obtained by dilution of the original sample in acetone. The single-walled carbon nanotubes used in this study were produced through the arc discharge method and have a diameter distribution in the range 1.0 ± 0.1 nm.

SERS experiments were obtained under microconditions by using silver colloidal solutions that were obtained by chemical reduction following the Lendl and Leopold method.[9] The resulting Ag nanoparticles had a diameter oscillating between 50 and 70 nm as reported previously.[10] For the measurements a droplet of this colloidal sample was evaporated on a glass slide, giving rise to a fractal colloidal silver structure. The nanotubes were deposited on that surface from a dispersion prepared by sonication of the nanotubes suspended in acetone. This procedure facilitates the nanotube surface interaction. Then, the required PYR analyte solutions (20 μL of 10^{-5} and 10^{-9} M PYR solutions) were dropped on the functionalized surface. Finally, the solvent was completely evaporated. The experimental setup of this micro-SERS device was explained in detail elsewhere.[7]

The Raman and SERS experiments were performed under ambient conditions using a backscattering configuration. The SERS and SERRS spectra were recorded with a Renishaw Raman Microscope System RM2000 equipped with a diode laser (providing a 785 nm line), an Ar^+ laser, providing the line at 514.5 nm, a Leica microscope and an electrically refrigerated CCD camera, and a notch filter to eliminate the elastic scattering. The spectra were obtained by using a 100× objective. The output laser power was 2.0 mW. Spectral resolution was 2 cm^{-1}.

Theoretical Methods, Molecular Models, and Calculations

The (5,5) armchair metallic single-walled nanotube and the pyrene were generated with the Hyperchem package, used for all the calculations. Before including the Ag surface, the following systems were generated to study their interaction in vacuo: nanotube/pyrene (S1) and two nanotubes/pyrene (S2). These configurations were chosen among several configurations considered for the whole interacting system for the molecular model calculation because they displayed the highest relative stability. Figure 1 shows some configurations for the S1 and S2 systems. In the S1 system the pyrene molecule is situated over the nanotube wall and parallel to it.

The silver surfaces were simulated as follows. A face-centered-cubic structure with $a = 0.408$ nm and $9 \times 9 \times 2$ cells was built. The resulting structure was trimmed to get a planar double layer of Ag composed of 324 atoms (surface A). The Ag surface simulating inhomogenities was simulated by trimming an original structure composed of $9 \times 9 \times 9$ cells giving a final surface model composed of 320 Ag atoms (surface B, Figure 2).

The next step was to generate the following models for the interaction of the pyrene and nanotubes with the Ag surface: two nanotubes/surface A (S3), pyrene/nanotube/surface A (S4), pyrene/two nanotubes/surface A (S5), and pyrene/two nanotubes/surface B (S6). S6 is shown in Figure 2.

In each model in which pyrene appeared all the possible stable configurations were considered. Given the size of these systems, we employed molecular mechanics to fully optimize the geometry in all cases. For the interaction of the nanotubes and pyrene with the Ag surfaces, the geometry of the latter was kept fixed during all calculations.

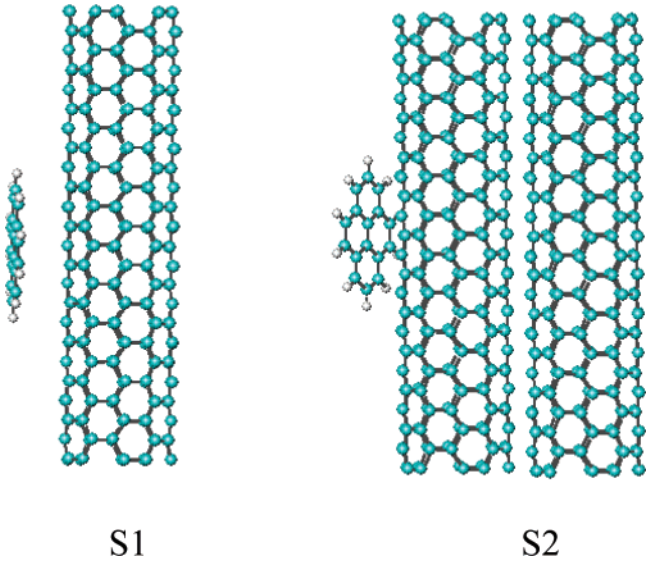

Figure 1. Molecular model for the nanotube/pyrene (S1) and two-nanotube/pyrene (S2) systems.

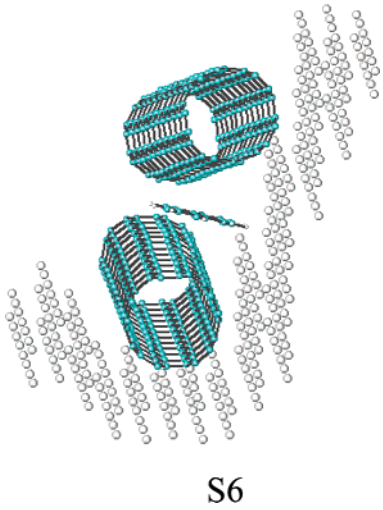

Figure 2. Molecular model for pyrene interacting with the nanotube functionalized inhomogenic silver surface B, system S6.

The wave functions for S1−S6 and for surfaces A and B were obtained with the extended Hückel method due to their size; this method has been successfully employed in our previous work on fullerenes and nanotubes.[11] Extended Hückel calculations produce qualitative or semiquantitative descriptions of molecular orbital and electronic properties.

Results and Discussion

Resonance Raman and SERRS Spectra of Nanotubes. The Raman resonance intensity depends on the density of the electronic states available for the optical transitions. In the case of single-walled nanotube bundles, only for those nanotubes having the valence and conduction band energy gap in resonance with the laser energy excitation will the Raman lines be observed with the highest intensity.

Figure 3 displays the resonance Raman spectra of the nanotubes obtained at different excitation wavelengths. The asymmetric broadness of the line at 1540 cm^{-1} obtained with the 514.5 nm excitation (2.41 ev) is characteristic of a G^- band of a metallic nanotube, which is consistent with the expected

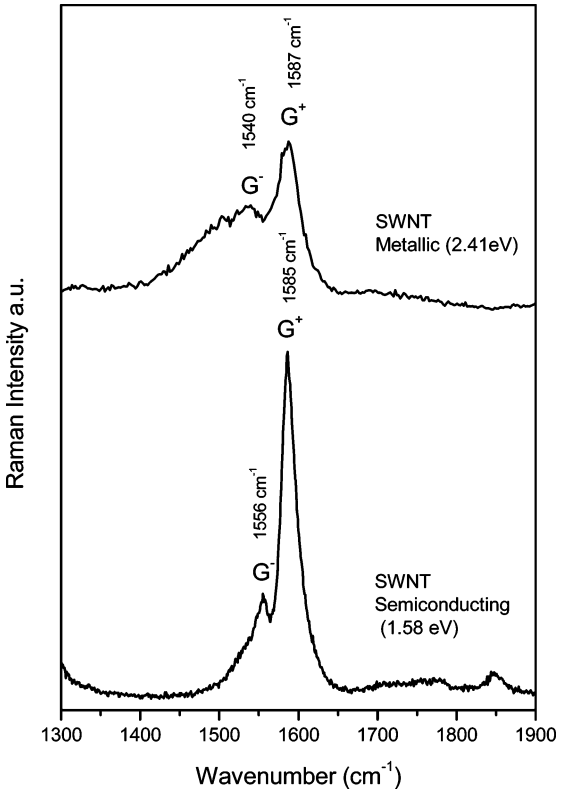

Figure 3. Raman spectra of nanotubes in the 1300−1900 cm^{-1} spectral region.

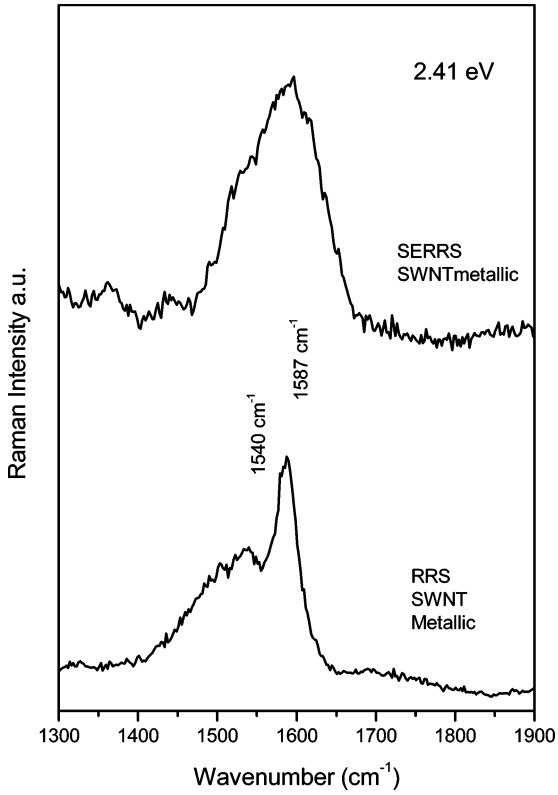

Figure 4. Raman resonance and SERRS spectra of nanotubes in the 1300−1900 cm^{-1} spectral region, irradiated with the 514.5 nm laser line.

Breit−Wigner−Fano (BWF) line shape. This band with the characteristic Lorenzian shape is drastically less intense when irradiating with the 785 nm laser line (1.58 ev), which indicates the presence of semiconducting species. The low relative intensity of the band at 1540 cm^{-1} suggests a small amount of that species in the sample. Both spectral behaviors are consistent with single-walled nanotubes.

The observed spectral difference of the G^- band by different excitation energy effects (1556 cm^{-1} at 785 nm and 1540 cm^{-1} at 514.5 nm) suggests the coexistence of nanotubes with different diameters. The fact that the G^+ band frequency is practically invariant by the same effect corroborates this proposition. The observed G^+-G^- difference indicates that the diameter of the metallic species is smaller than the diameter of the semiconducting species.

The Raman spectrum and the surface-enhanced resonance Raman spectrum of the nanotubes excited by the 514.5 nm laser line are displayed in Figure 4. The main spectral feature concerns the G^+ band, which broadens by surface effect. This behavior is characteristic of metallic nanotubes, and it is the result of a significant perturbation of the electronic levels of the adsorbed nanotubes. These results are explained in terms of a charge transfer between the nanotube and the silver surface, as proposed by Corio et al. in related systems deposited on several surfaces.[8] In the case of semiconducting nanotubes, normal resonance Raman and SERRS spectra profiles are very similar.

The Pyrene/Nanotube/Silver Surface Interaction. The Raman spectrum of the analyte pyrene, the SERRS spectrum of the assembler metallic single-walled nanotube, and the SERS spectrum of the pyrene/nanotube system deposited on the silver surface, all of them obtained by exciting with the 514.5 nm laser line, are displayed in Figure 5. No significant bands were observed in the spectrum of the nanotube below 1500 cm^{-1} (Figure 5d), which facilitates the identification of the analyte. The SERS spectra of the pyrene adduct display all the pyrene

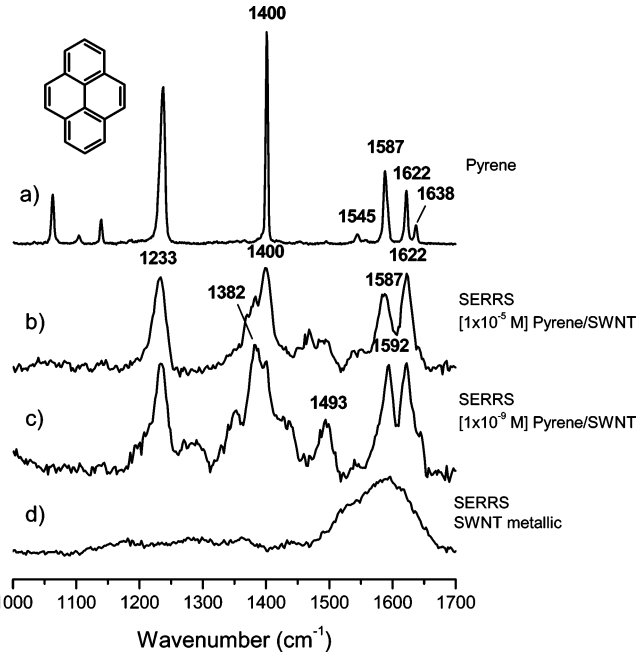

Figure 5. (a) Micro-Raman spectrum of solid pyrene, (b, c) micro-SERRS spectra of pyrene on a nanotube/silver surface at two concentrations, and (d) micro-SERRS spectrum of nanotube, all in the 1000−1700 cm^{-1} spectral region and exciting at 514.5 nm.

bands at concentrations as low as 10^{-9} M (Figure 5b). A simple calculation made by taking into account that at this pyrene concentration the surface density of analyte is 437 molecules/μm^2 and that the total analyzed area is 0.78 μm^2 (if considering a laser spot of 1 μm diameter) points out that the total number of pyrene molecules analyzed in the case of adding the 10^{-9} M solution is 343. This is probably still far from the single-

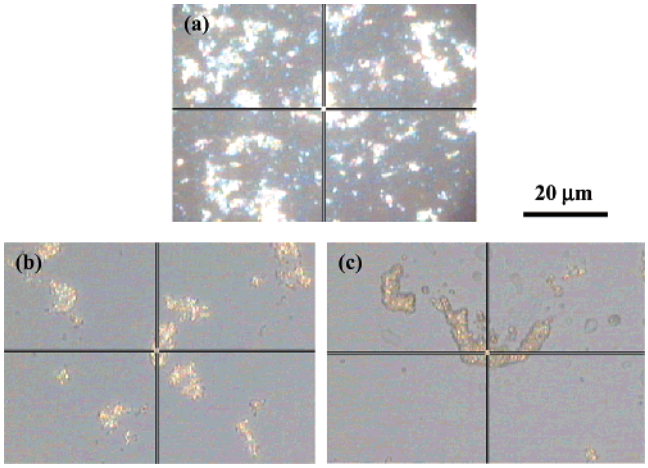

Figure 6. Optical micrographs of the Ag nanoaggregates employed to record micro-SERRS spectra: (a) in the absence of adsorbate; (b, c) different regions of the immobilized Ag nanoaggregates obtained in the presence of NT/pyrene complex. The crossing point corresponds to the one where the SERRS spectra were recorded.

molecule detection referred to previously for very active SERS molecules, but it is a very satisfactory result if one considers that pyrene is not active under the point of view of SERS effect.

The SERS of pyrene at 10^{-5} M (Figure 5c) shows marked changes in both the intensity of bands and the peak positions in comparison to the Raman of the solid pyrene (Figure 5a). These changes are much stronger at the lowest concentration (10^{-9} M) (Figure 5b). This is probably due to the higher analyte dispersion on the exposed surface which induces the formation of a monolayer on the nanotube surface where the molecules adopt a particular orientation. Another surface effect observed on these surfaces is a general broadening of bands suggesting the existence of a charge transfer between the analyte and the nanotube/metal system, which stabilizes the nanotube−pyrene interaction.

As concerns the band intensities, the band at 1622 cm^{-1} is markedly enhanced, most probably due to a resonant effect induced by the charge-transfer complex formed with the nanotube. In addition, the 1587/1622 cm^{-1} ratio is inverted. These changes also occur in the SERS of calixarene/pyrene complexes, and were also attributed to such an interaction.[4] However, contrary to what happens in the presence of calixarene, pyrene main bands almost do not change their positions. Thus, we have deduced that the interaction strength is lower in the case of the complex with the nanotube. The new bands at 1493, 1468, and 1382 cm^{-1} could be due to impurities existing in the medium.

By pyrene concentration decreasing (from 10^{-5} to 10^{-9} M), the band at 1587 cm^{-1} undergoes a significant shift to 1592 cm^{-1}, and the band at 1400 cm^{-1} becomes weaker. This could be an effect of a tighter interaction of the analyte with the nanotube at lower concentrations.

The in-plane C−H bending bands in the 1200−1000 cm^{-1} region almost disappear due to the surface effect. This is attributed to a parallel orientation of pyrene on the nanotube surface.

Figure 6 shows the optical micrographs of the samples employed to record the micro-SERRS spectra. As can be seen, the color of the nanoaggregates changes significantly in the aggregates containing NT (Figure 6b,c) in relation to those in the absence of NT (Figure 6a), thus demonstrating the adsorption of NT on the metallic surface. In certain regions a thick black layer can be seen surrounding the nanoaggregates (Figure 6c).

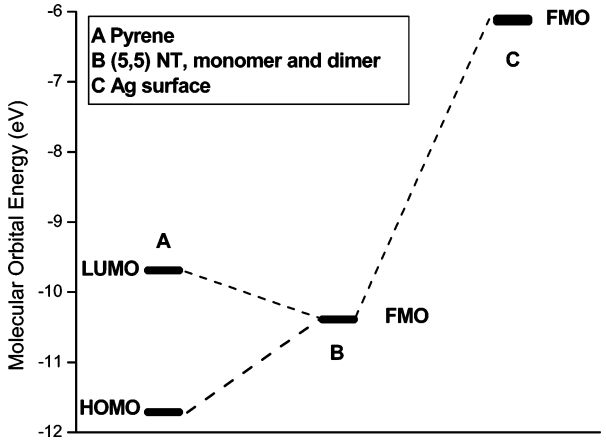

Figure 7. Energy diagram for pyrene, nanotubes, and the silver surface. FMO, frontier molecular orbitals, corresponding to HOMO and LUMO.

Theoretical Results. In all calculations the final pyrene−nanotube and nanotube−nanotube distances are about 3.40 Å, which is almost the same as that observed between graphite layers (3.41 Å). The minimal nanotube−silver surface distances is 3.6 Å.

The extended Hückel calculation for the S1 system indicates a small amount of charge transfer from pyrene to NT (0.001 e); this is due to the fact that the carbon atoms composing the central part of the nanotube have a small positive net charge. Calculations of systems S3−S6 show a charge transfer from the surface toward the nanotubes. These results can be rationalized by inspecting Figure 7.[12] In fact, it can be seen that there is no favorable charge transfer from pyrene to the nanotube because there is a 1.42 eV gap between the pyrene highest occupied molecular orbital (HOMO) and the nanotube lowest unoccupied molecular orbital (LUMO), with the latter having a higher energy.

A very interesting result emerges for system S2 (Figure 1). Here, there is no charge transfer from the pyrene to the NT closer to it. Nevertheless, there is a substantial charge transfer (1.94 e) from the NT closer to pyrene toward the other NT. This high value could be explained by considering that the NT displays a bundle distribution with a charge distributed among all the partners. By considering pyrene as a perturbation, it is possible to propose that this polarization of the nanotubes is why they form bundles in aromatic solvents.[13]

The Ag surface A (planar) has a HOMO with energy of −6.14 eV and a LUMO with energy of −6.13 eV. Surface B, with less symmetry than surface A, has a HOMO with energy of −6.27 eV and a LUMO with energy of −6.26 eV. Figure 7 shows that the Ag surface HOMO is located 4.25 eV above the LUMO of the nanotube. These results suggest that, independent of the surface geometry, the charge transfer is highly favored from the Ag surface toward the NT, thus confirming the experimental results.

Conclusions

It has been demonstrated that metallic single-walled carbon nanotubes can be used as molecular assemblers between a silver colloid surface and the analyte pyrene. The SERS effect allows the detection of pyrene at concentrations in the limit of 10^{-9} M. The SERS spectral analysis indicates that the pyrene−nanotube interaction occurs through a $\pi-\pi$ stacking. The interaction mechanism involves a charge transfer from the Ag metal surface to the pyrene−nanotube complex. Theoretical results based on simplified molecular models in which the

nanotubes were considered as being single-walled units with metallic characteristics fully agree with experimental results. On the whole our results suggest that nanotubes could be used as molecular assemblers in optical sensor devices to detect PAHs.

Acknowledgment. We acknowledge Dr. Teresa de los Arcos for providing the nanotubes, and also the following grants: Project Fondecyt 1040640 from Conicyt (Chile), the Convenio Conicyt/CSIC 2003/2004, Fundación Andes Project No. C-13879, Grant FIS2004-00108 from Dirección General de Investigación, Ministerio de Educación y Ciencia, and the GR/MAT/0439/2004 and S-0505/TIC/0191 (MICROSERES) grants from Comunidad Autonoma de Madrid. P.L. acknowledges Project No. AT 4040084 from Conicyt.

References and Notes

(1) Star, A.; Han, T.-R.; Gabriel, J.-C. P.; Bradley, K.; Grüner, G. *Nano Lett.* **2003**, *3*, 1421

(2) Zhang, J.; Lee, J.-K.; Wu, Y.; Murray, R. W. *Nano Lett.* **2003**, *3*, 403.

(3) Chen, R. J.; Zhang, Y.; Wang, D.; Dai, H. *J. Am. Chem. Soc.* **2001**, *123*, 3838.

(4) Nakashima, N.; Tomonari, Y.; Murakami, H. *Chem. Lett.* **2002**, *6*, 638.

(5) Lee, M. L.; Novotny, M.; Bartle, K. D. *Analytical chemistry of polycyclic aromatic compounds*; Academic Press: New York, 1981.

(6) Carrasco, E. A.; Campos-Vallette, M.; Inostroza, N.; Leyton, P.; Diaz, F. G.; Clavijo, R. E.; García-Ramos, J. V.; Domingo, C.; Sanchez-Cortes, S.; Koch, R. *J. Phys. Chem. A* **2003**, *107*, 9611.

(7) Leyton, P.; Sanchez-Cortes, S.; Garcia-Ramos, J. V.; Domingo, C.; Campos-Vallette, M. M.; Saitz, C.; Clavijo, R. E. *J. Phys. Chem. B* **2004**, *108*, 17484.

(8) Corio, P.; Brown, S. D. M.; Marucci, A.; Pimenta, M. A.; Kneipp, K.; Dresselhaus, G.; Dresselhaus, M. S. *Phys. Rev. B* **2000**, *61*, 13202.

(9) Lendl, N.; Leopold, B. *J. Phys. Chem. B* **2003**, *107*, 723.

(10) Cañamares, M. V.; Garcia-Ramos, J. V.; Gómez-Varga, J. D.; Domingo, C.; Sánchez-Cortes, S. *Langmuir* **2005**, *21*, 8546.

(11) Gómez-Jeria, J. S.; Gónzalez-Tejeda, N.; Soto-Morales, F. *Bol. Soc. Chil. Quím.* **2003**, *48*, 85.

(12) Fleming, I. *Frontier Orbitals and Organic Chemical Reactions*; John Wiley & Sons: New York, 1998.

(13) Bahr, J. L.; Mickelson, E. T.; Bronikowski, M. J.; Smalley, R. E.; Tour, J. M. *Chem. Commun.* **2001**, 193.